Light-Dependent OCT Structure Changes in Photoreceptor Degenerative rd 10 Mouse Retina

Yichao Li,[1] Yikui Zhang,[2] Sonia Chen,[1] Gregory Vernon,[*,1] Wai T. Wong,[2] and Haohua Qian[1]

[1]Visual Function Core, National Eye Institute, National Institutes of Health, Bethesda, Maryland, United States
[2]Unit on Neuron-Glia Interactions in Retinal Disease, National Eye Institute, National Institutes of Health, Bethesda, Maryland, United States

PURPOSE. Using optical coherence tomography (OCT) to analyze the effects of light/dark adaptation in a mouse model of inherited photoreceptor degeneration (rd10), and to study dynamics of subretinal fluid during the progress of retinal degeneration.

METHODS. rd10 and wild-type (WT) C57BL/6J mice were reared in cyclic light or darkness and imaged with Bioptigen UHR-OCT or Spectralis HRA+OCT after adaptation to either light or darkness.

RESULTS. OCT images from rd10 mice were analyzed at three progressive stages of degeneration. After light-adaptation, stage I (postnatal age [P]26–29) eyes demonstrated no apparent subretinal fluid. At stage II (P32–38), subretinal fluid was present and restricted to parapapillary area, while at stage III (P44–45) extensive subretinal fluid was present across many retinal areas. Following overnight dark-adaptation, WT eyes showed a large reduction in outer retinal thickness (4.6 ± 1.4 μm, $n = 16$), whereas this change was significantly smaller in stage I rd10 eyes (1.5 ± 0.5 μm, $n = 14$). In stage II rd10 eyes, dark-adaptation significantly reduced the extent of subretinal fluid, with the amount of reduction correlating with the amount of fluid pre-existing in the light-adapted state. However, dark-adaptation did not significantly alter the amount of subretinal fluid observed in stage III rd10 mice. In addition, dark-rearing of rd10 mice from P6 to P30 slowed retinal degeneration.

CONCLUSIONS. Visual experience in the form of light/dark adaptation exerts a significant effect on outer retinal structure in the context of photoreceptor degeneration. This effect may arise from light-dependent alterations in fluid transport across the RPE monolayer, and promote photoreceptor survival as induced by dark-rearing.

Keywords: optical coherence tomography, retinal degeneration, mouse, rd10, subretinal space

Optical coherence tomography (OCT) is a noninvasive in vivo imaging method that can provide high-resolution optical section of the tissue, and has been widely used in the diagnosis and monitoring of retinal disease in the clinic and the laboratory.[1–3] In addition to providing structural information on retinal anatomy, OCT can also be used to perform time-lapse imaging of the retina to discover dynamic morphological changes in response to light stimulus.[4–9] As the light source used for OCT imaging usually lies in the infrared spectrum beyond the detection range of the eye, it can be used to measure changes in retinal structure in response to visible light without interfering of light responses. We had recently reported the phenomenon of light-dependent dynamic changes in retinal thickness in the wild-type (WT) mouse retina using ultra-high resolution OCT.[4] Specifically, light-adaptation elicits an increase of the outer retinal thickness with the induction of an additional hypo-reflective band between RPE and photoreceptor tip (PRT) layers. It is proposed that this light-dependent OCT response is mediated by dynamics of subretinal fluid, most likely through light-sensitive regulation of RPE pump activities.[4,10]

Although light-induced accumulation of subretinal fluid has been well-documented in animal studies,[11–16] the effect of photoreceptor degeneration such as that occurring in retinitis pigmentosa (RP) on subretinal fluid is largely unexplored. As the integrity of subretinal space is essential to maintain proper function for photoreceptors and RPE, understanding the influence of photoreceptor degeneration on subretinal fluid regulation can help to provide insight into the pathophysiology in RP and may translate to new therapeutic approaches for this blinding disease.

In this study, we examined OCT images under light- and dark-adapted conditions of commonly studied rd10 mouse model of RP, and tested hypothesis that light-dependent OCT changes in outer retina thickness is mediated by the dynamics of subretinal fluid in the eye. This mouse line contains a homozygous point mutation in the rod photoreceptor-specific *Pde6b* gene,[17,18] which leads to progressive photoreceptor degeneration. Mutations in the same gene have also been found in human RP patients.[19] As a commonly used RP model, the time course of the photoreceptor degeneration and cellular changes in the retina for rd10 mice have been well documented.[11,20–24] In addition, it has been reported that rd10 mice develop retinal separation from RPE layer during the course of retinal degeneration, suggesting an accumulation of subretinal fluid.[11] Therefore, rd10 mice provide a suitable

model to examine the link of light-dependent OCT structure changes and subretinal fluid dynamics in the eye and to investigate the effects of retinal degeneration on subretinal fluid regulation. Here, we report that light-dependent changes in outer retina thickness are maintained in rd10 retina but vary with the stage of degeneration and with the amount of pre-existing fluid in the subretinal space.

METHODS

Experimental Animals

All procedures involving animals were conducted under an approved National Institutes of Health animal care protocol, and all animals were treated in accordance with the ARVO Statement for the Use of Animals in Ophthalmic and Vision Research. Mice (C57BL/6J and rd10) were kept in regular animal housing under a 50lux 14:10-hour light/dark cycle. In addition, a subgroup of rd10 mice were dark reared.

OCT Imaging

Mice were anesthetized with ketamine (100 mg/kg) and xylazine (6 mg/kg). OCT images were captured using either Envisu UHR2200 (Bioptigen, Durham, NC, USA) or Spectralis (Heidelberg Engineering, Franklin, MA, USA). Whereas Envisu system employs a wider bandwidth (160 nm) for OCT beam and provides a higher axial resolution (1.6 μm in tissue), the Spectralis instrument combines simultaneous reflectance fundus imaging with OCT imaging, which allows for precise and repeatable scanning at the same retinal region during follow-up studies. Light-adapted animals were imaged in the procedure room under standard illumination conditions (500lux). Dark-adapted animals were prepared under dim red light and imaged in darkness. For Bioptigen Envisu system with a 50-degree OCT field, mouse eye was positioned with the optic nerve head (ONH) in the center of the OCT scan. Full field volume scans (1.4 mm × 1.4 mm at 1000 A-scan × 100 B-scan × 5) were captured. In addition, two radial scans were acquired at horizontal and vertical position and averaged 40 times. For Heidelberg Spectralis system with a 30-degree OCT field, volume scans of nasal and temporal side of ONH were captured with each B-scan averaged 30 times.

Dark Rearing

Dark rearing was commenced in rd10 animals at postnatal age (P) 6 by moving pre-weaning litters and their dams to darkened, light-shielded housing. Animal husbandry was performed under dim red-light illumination. At P30, OCT images were captured with Spectralis, along with nondark reared control animals housed under normal cyclic light condition.

OCT Image Analysis and Measurements

For OCT images captured by Bioptigen Envisu system, averaged radial scan images were used for retinal thickness measurement. For each eye, measurements were performed on four spots (450 μm from center of ONH at both horizontal and vertical directions) using vendor provided Reader program (Bioptigen), and the averaged number was used as the measurement for the eye. Total retina thickness was measured from nerve fiber layer (NFL) to basal side of RPE layer (Bruch's membrane [BM]). Outer retina length was measured from outer limiting membrane (OLM) to BM, two clearly distinguishable OCT layers even for degenerative retina. The same four spots were also used to calculate intensity profile across

the outer retina based on averaged value of 10-pixel width at the spot center of OCT images. The width of EZ (IS/OS) (the inner segment ellipsoid zone, also referred as the inner segment/outer segment [IS/OS] junction[10,25–27]) was calculated from mid-point of ascending and descending phases on intensity profile of the band (as illustrated in Fig. 1). For OCT images captured with Heidelberg Spectralis, the frame of OCT B-scan that showed the largest subretinal fluid accumulation from each eye was selected for analysis. The highest values of outer retina length (from OLM to BM) were measured. Data are presented as mean ± SEM.

RESULTS

As there are progressive changes of subretinal fluid accumulation in rd10 mice,[11] we divided these mice into three stages across the course of photoreceptor degeneration: stage I, ranging from P26 to P29, during which no apparent subretinal fluid was observed; stage II, ranging from P32 to P38, during which some patchy subretinal fluid accumulation restricted to the central retina; and stage III, ranging from P44 to P48, during which subretinal fluid accumulation extending over large areas of the retina.

rd10 Mice at Stage I of Degeneration Demonstrate an Outer Retinal Thickening in Response to Light-Adaptation That Is Much Smaller Than That Observed in WT Mice

We evaluated rd10 mice during stage I (at P26–P29) and WT mice using OCT and compared retinal thickness changes between light-adapted and dark-adapted (overnight dark adaptation) in these two groups. Even at this early stage, rd10 retina has undergone significant photoreceptor degeneration,[18,20,24] resulting in marked retinal thinning relative to WT retina (Fig. 1) that arose primarily from outer retinal atrophy. Averaged total retina thickness for WT and rd10 mice are summarized in Figure 2A, and values for outer retina thickness (OLM to BM) for WT and rd10 are shown in Figure 2B.

As previously reported for WT retina, light adaptation induced changes in OCT images with appearance of a hypo-reflective zone between PRT and RPE layer (pointed by red arrows in Fig. 1A) that lead to an increase in retina thickness.[4] This increase of retinal thickness under light-adapted conditions can be detected in both total retinal thickness and outer retina thickness measurements (Figs. 2A, 2B). In addition, Zhang et al.[9] recently reported that high intensity light adaptation induced a number of changes in OCT bands in outer retina. In particular, the intensity of EZ (IS/OS)[10,25–27] was increased after light stimulation. To better characterize the light-induced changes in OCT image, we plotted intensity profile of outer retina as shown in lower panel of Figure 1. Measured band thickness and peak intensity of EZ (IS/OS) zone are summarized in Figures 2D and 2E, respectively. For WT retina, there is a significant reduction in EZ (IS/OS) zone thickness and small reduction in peak intensity (although statistically not significant) of OCT images captured under dark-adapted conditions.

In addition to the reduction of total retina thickness and outer retina thickness, OCT images of rd10 retina also revealed other differences in outer retina in this degenerative retina (Fig. 1B). For stage I rd10 retina, only three layers (OLM, EZ [IS/OS], and RPE) are distinguishable on OCT images, as illustrated on intensity plot in Figure 1B. EZ (IS/OS) zone is much thinner (Fig. 2D), and the peak intensity is slightly weaker (Fig. 2E) as compared with OCT images from WT retina. For stage I rd10 mice, small but statistically significant changes in retinal
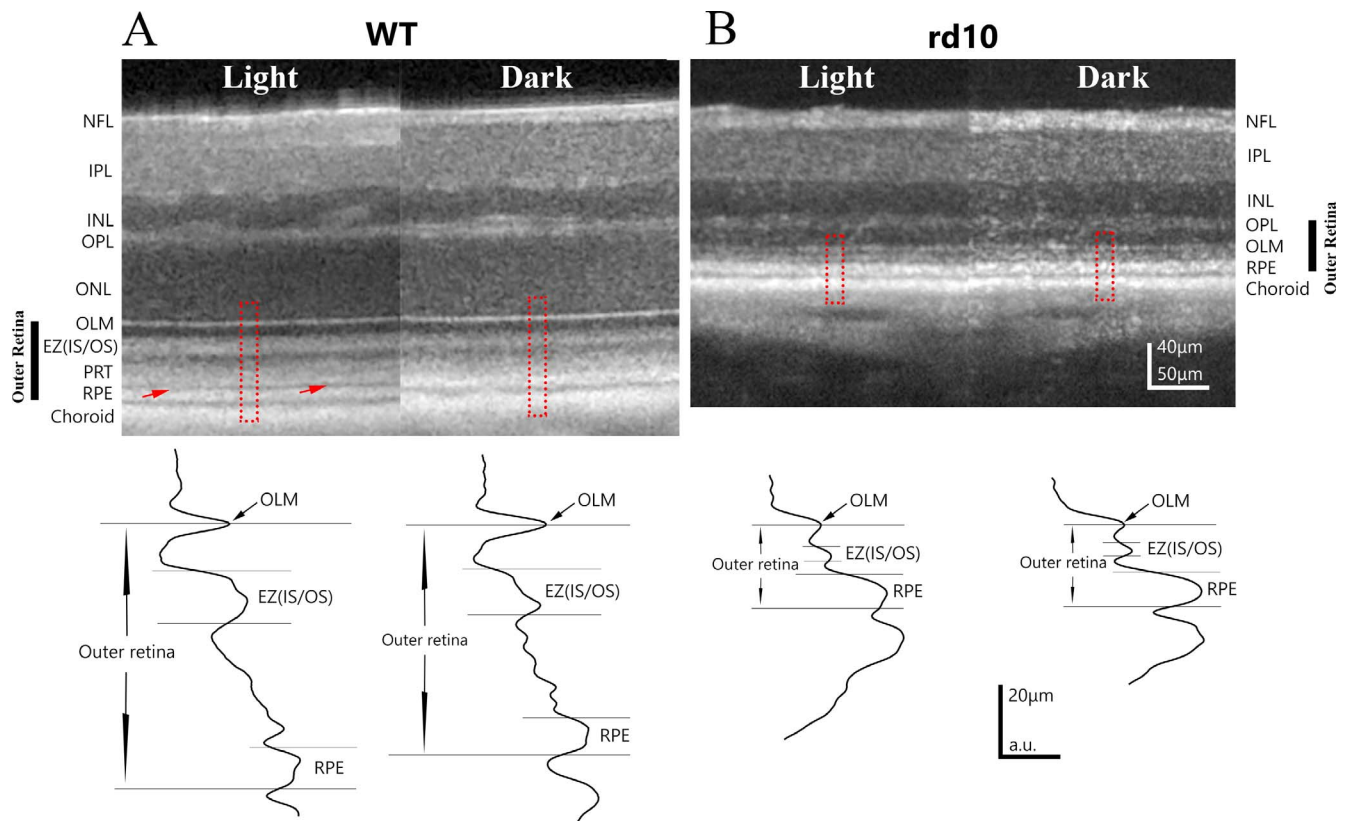
FIGURE 1. Examples of OCT images obtained from light- and dark-adapted WT and stage I rd10 mice. (**A**) Representative example of OCT retinal images obtained from the same eye of a P40 WT mouse under light-adapted and dark-adapted conditions. *Red arrows* point to a hyporeflective layer between PRT layer and RPE layers, which is present under light-adapted conditions but absent in dark-adapted conditions. Intensity profiles for outer retina region (outlined by *red dash line box*) are shown in the *bottom panel*. (**B**) Representative example of OCT retinal images obtained from the same eye of a P26 rd10 mouse under light-adapted and dark-adapted conditions. Light-induced OCT response is much smaller in this stage I rd10 mouse. *Bottom panel* illustrates intensity profile of OCT intensity in outer retina from outlined regions. NFL, nerve fiber layer; IPL, inner plexiform layer; INL, inner nuclear layer; OPL, outer plexiform layer; ONL, outer nuclear layer.

thickness could also be detected when comparing OCT images obtained from light- and dark-adapted conditions (Figs. 1B, 2A, 2B). Specifically, light adaptation slightly increased outer retina thickness. However, the magnitude of this light-induced increase was markedly and significantly smaller than those observed in WT mice, with a total mean increase that was only approximately one third of that in WT mice (Fig. 2C). In addition, dark-adaptation does not elicit any significant change of EZ (IS/OS) zone for either band thickness (Fig. 2D) or peak intensity (Fig. 2E).

Subretinal Fluid Accumulation Changes in Light-Adapted Stage II rd10 Retina Undergoes Resolution During Dark Adaptation

Under light-adapted conditions, rd10 retinas during stage II (P32–P38) demonstrated patchy subretinal fluid accumulation between photoreceptor and RPE layers, leading to areas of separation of neural retina from the RPE[11] that typically occurred in the superotemporal quadrant of the central retina. A representative example of horizontal B-scan OCT images of a stage II rd10 retina is shown in Figure 3A. Interestingly, following overnight dark adaptation, these areas of subretinal fluid largely resolved. Magnified images illustrate subretinal fluid accumulation and absorption under light- and dark-adapted conditions are shown in Figure 3B, along with intensity profile of outer retina region on the right-side panel. For stage II rd10 retina, only OLM and RPE

bands are clearly resolvable in outer retina, and distance between these bands (outer retina thickness) is much larger under dark-adapted condition than those observed under dark-adapted retina.

Figure 3C shows quantitative measurement of outer retina thickness of stage II rd10 eyes. Due to the accumulation of subretinal fluid, the mean outer retina thickness (from OLM to BM) under light-adapted conditions is even greater than that found in stage I rd10 retinas (36.9 ± 2.5 μm, $n = 11$, compared to 22.1 ± 0.7 μm, $n = 16$; $P = 5 \times 10^{-7}$, unpaired t-test). With the resolution of this subretinal fluid with overnight dark-adaptation, the mean change in outer retinal thickness in stage II eyes exceeded that in stage I eyes (6.7 ± 1.0 μm compared to 1.4 ± 0.4 μm; $P = 4 \times 10^{-5}$, unpaired t-test).

As there was considerable variation in the thickness of the layer of subretinal fluid in individual stage II rd10 eyes, and in between different retinal regions in the same eye, we investigated the relationship between fluid accumulation and the light-induced changes in outer retina thickness. Results are summarized in Figure 3D, where each point represents one measurement on the OCT images (i.e., four points for each eye, two from nasal and temporal field of horizontal B-scan, and two from superior and inferior field of vertical B-scan). The data could fit with a linear equation ($R^2 = 0.84$) between the outer retina thickness measured from light-adapted OCT image and the light-dependent changes in outer retinal thickness. The fitted line has x-intercept (green arrow) of 22.27 μm, a value that most likely reflects outer retina thickness when no
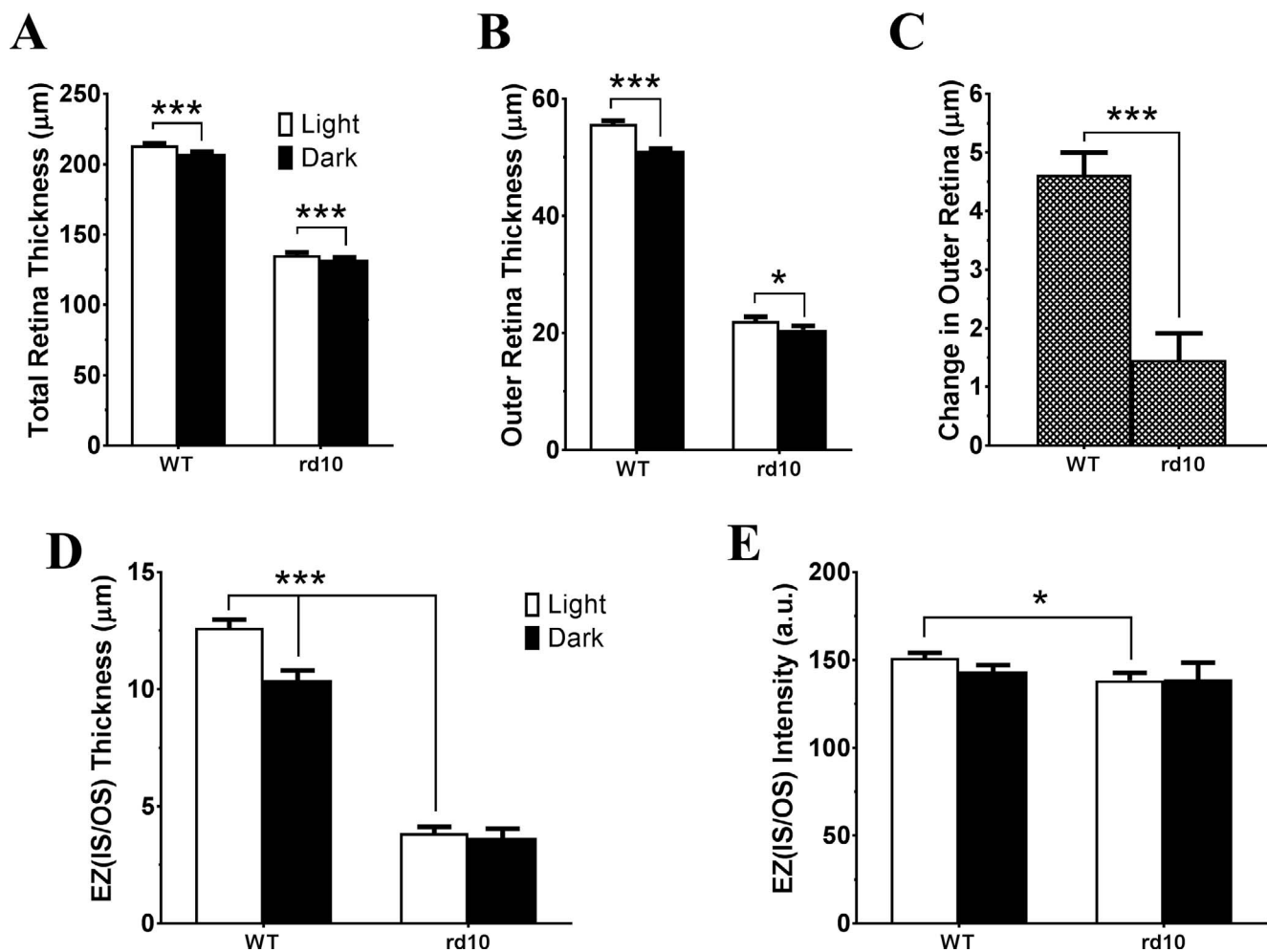
FIGURE 2. Light-induced OCT responses in WT and stage I rd10 mice. *Bar graphs* summarized measurements from OCT images acquired under light- and dark-adapted conditions of WT and rd10 eyes for averaged total retinal thickness (**A**), outer retinal thickness (**B**), light-adaptation induced OCT responses (**C**), EZ (IS/OS) thickness (**D**), and EZ (IS/OS) peak intensity (**E**). $N = 16$ for WT and $N = 14$ for rd10. $*P < 0.05$; $***P < 0.001$. (**A**, **B**, **D**: paired *t*-test; **C**, **E**: unpaired *t*-test).

subretinal fluid is present. This is very similar as the outer retina thickness observed on stage I rd10 mice (22.1 ± 0.7 μm, Fig. 2B). The slope of regression line is 0.84, which is smaller than unity, indicating that dark-adapted retina does not completely remove the accumulation of subretinal fluid observed under light-adapted status.

As accumulation of subretinal fluid demonstrated regional variations in stage II rd10 eye, differences in scan position could affect the values of outer retina thickness measured under light- and dark-adapted conditions. Therefore, the comparison would be more accurate if the scan was performed at the exact retinal position under both conditions. Spectralis system (Heidelberg Engineering) has capacity of performing follow-up OCT images at the exact same retinal location using fundus image as a reference during eye tracking. An example of initial OCT scan under light-adapted condition from a stage II rd10 mouse eye is shown in Figure 4A (top panel). The example of B-scan OCT image was selected to have the largest subretinal fluid accumulation (pointed by red arrows) among all volume OCT scan performed on the eye. The follow-up image after overnight dark-adaptation from the same retinal spot is shown at bottom panel of Figure 4A. Clearly, the subretinal fluid is mostly dissolved after overnight dark-adaptation. Figure 4B shows magnified OCT images from light- and dark-adapted conditions (portion outlined by blue lines in

Fig. 4A) with intensity profile of outer retina shown on the right-side panel. Similar as OCT images captured with Bioptigen OCT system, only OLM and RPE bands are clearly resolvable in outer retina for stage II rd10 mice on images obtained with Spectralis. The OLM band is relatively larger on Spectralis OCT image (Fig. 4B) than those captured with Bioptigen OCT system (Fig. 3B), most likely due to relatively lower axial resolution of Spectralis system to resolve OLM from residual degenerative photoreceptor. Large accumulation of subretinal fluid is easily distinguishable on the OCT image captured under light-adapted condition. The amount of subretinal fluid is greatly reduced after overnight dark-adaptation at the same retinal location, although there are still some residual left. We quantitated the outer retina length under these two conditions, and results are shown in Figure 4C.

The correlation between light-adapted outer retina thickness and changes induced by dark-adaptation is shown in Figure 4D. In this plot, data from each eye is represented by one point. The results could fit with a linear equation ($R^2 = 0.44$) with x-intercept of 22.41 μm, a value similar as the outer retinal thickness for stage I rd10 mice (Fig. 2B). The regression line has a slope of 0.4, suggesting less effectiveness of dark-adapted retina for removing subretinal fluid in this group of rd10 mice.
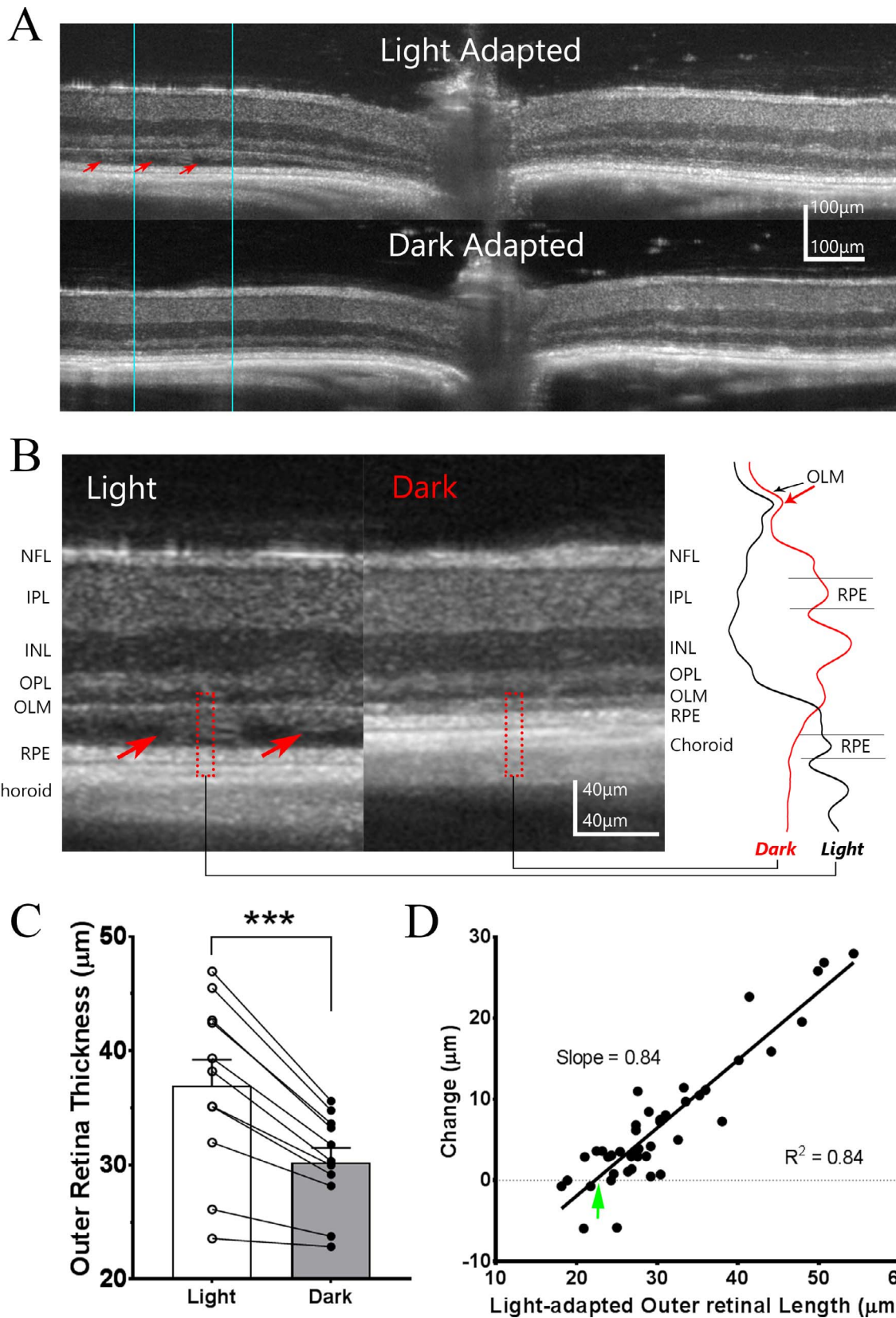
FIGURE 3. Light adaptation induces subretinal fluid accumulation in rd10 mice during Stage II of degeneration. (**A**) Representative example of OCT images obtained from the same P34 rd10 mouse retina under light-adapted and dark-adapted conditions. Areas of subretinal fluid accumulation (*red arrows*) can be observed under light-adapted conditions but these fully resolve following overnight dark-adaptation. (**B**) Side-by-side comparison of the OCT images at high magnification for the same local retina region outlined by *blue lines* in [**A**]. Intensity profiles for outer retina region outlined by *dash red box* are shown on the *right-side panel*. *Red arrows* point to the fluid accumulation in subretinal space under light-adapted condition, which is largely resolved following dark adaptation. (**C**) Change in outer retinal thickness for stage II rd10 retinas ($n = 11$) under light and dark-adapted

conditions. (**D**) Relationship between the change in outer retina thickness between dark- and light-adapted conditions and outer retinal length observed under light-adapted conditions for individual measurements at each retinal locus ($n = 44$ measurements from 11 eyes of six animals; Pearson's correlation coefficient). *Green arrow* points to *X*-intercept, a value corresponds to the outer retina length with no subretinal fluid accumulation.

Subretinal Fluid in Stage III rd10 Mice Is Not Affected by Adaptation Status

With the progression of retinal degeneration along postnatal age, the extent of accumulated subretinal fluid between photoreceptor and RPE layer also increased. An example of OCT image from stage III rd10 mice (P44–P48) obtained under light- and dark-adapted conditions is shown in Figure 5A. The accumulation of subretinal fluid involved large areas, which extended across the width of individual OCT scans. Similar amounts of subretinal fluid were also observed on OCT image acquired after overnight dark-adaptation. Figure 5B shows magnified OCT images from light- and dark-adapted conditions (portion outlined by blue lines in Fig. 5A) with intensity profile of whole retina shown on the right-side panel. OLM and RPE bands are clearly visible in outer retina for stage III rd10 mice, although they are separated further apart by hypo-reflective fluid accumulated area. Quantitative measurements of outer retina length under light- and dark-adapted conditions are summarized in Figure 5C. The relationship between light-adapted outer retina thickness and light-induced OCT response is shown in Figure 5D. Each data point represents values derived from one mouse eye. For stage III rd10 mice, there is no correlation between outer retina length and the changes induced by adaptation, indicating that the amount of subretinal fluid in stage III rd10 mice was not affected by adaptation status.

Effect of Dark-rearing on Retinal Degeneration in rd10 Mice

Accumulation of subretinal fluid separates photoreceptors from RPE layer and reduces the support and protective function of RPE to photoreceptor cells. Therefore, subretinal fluid observed in rd10 mice under light-adapted condition could accelerate retinal degeneration in these animals. To test this hypothesis, we raised young rd10 pulps under total darkness starting at P6, and examined their retinal structure by OCT imaging at P30. Their littermates raised in normal light condition (i.e., 14:10 light/dark cycle) were used as controls. Figure 6A shows one example of OCT images from control eye and one from dark-reared rd10 mouse eye, with intensity profile of OCT images plotted on the right-side panel. The animals kept in dark exhibit much larger outer nuclear layer thickness than those of control, whereas inner retinal layers were very similar. In addition, dark-reared animals exhibit prominent EZ (IS/OS) zone, whereas OCT images obtained from control rd10 mice can only detect OLM and RPE bands in the outer retina region. Quantitative measurements from four control and four dark-reared mice are summarized in bar graphs shown in Figures 6B through 6D. Dark-reared mice exhibited significant higher in total retinal thickness than controls (Fig. 6B). The difference was mainly in photoreceptor layer, with significant thinning of ONL thickness for control retina (Fig. 6C). On the other hand, the thicknesses of the inner retina (from OPL to NFL) were similar for control and dark-reared mice (Fig. 6D). These results indicated a protective effect of dark-rearing on retinal degeneration in rd10 mice.

DISCUSSION

Light exposure induces a number of structural changes in the retina that can be detected by OCT imaging.[4,5,8–10] In WT mice

(Figs. 1A, 2), light-adaptation under the illumination of normal housing conditions induces an increase of outer retina thickness with appearance of an additional hypo-reflective layer separating PRT from RPE layers. In addition, light-adaptation induced a widening of EZ (IS/OS) zone on OCT images (Fig. 2D) and slight increase in peak intensity (Fig. 2E). These changes most likely reflect light-dependent alterations in fluid accumulation in subretinal space.[13–16,28] Correlation between light-dependent OCT changes in outer retina thickness and amount of subretinal fluid observed for stage II rd10 mice (Figs. 3, 4) provides additional support for this hypothesis. Recently, similar changes in outer retina thickness in response to intense flash light stimulation have been measured in mice and human eyes.[9,10] Unlike the current study that examined retina structure under steady light- and dark-adapted conditions, these reports monitored dynamic changes on OCT images following an intense flash light that bleaches significant amounts of rhodopsin. Differences in light stimulation might account, in part, for variations observed on magnitudes of outer retinal changes. In addition, Zhang et al.[9] used linear scale to quantitate OCT image, whereas most commercial instruments (including those used in this study) produce OCT images in logarithmic scale. Such scaling difference might contribute to different in EZ (IS/OS) zone intensities.

Stage I rd10 mice exhibited significant photoreceptor degeneration evident as large reduction in outer nuclear layer and outer retinal thickness (Figs. 1B, 2A, 2B). In addition, the EZ(IS/OS) zone is much narrower (Fig. 2D) and less intense (Fig. 2E) compared with WT controls. The EZ (IS/OS) zone was completely absent in Stage II rd10 mice (Figs. 3, 4) indicating further progression of photoreceptor degeneration. As photoreceptors degenerate, light-dependent OCT changes in outer retina were also significantly diminished (Figs. 1, 2). The RPE layer plays important roles in regulating fluid transfer in outer retina.[12,29–31] However, RPE cells themselves are not intrinsically sensitive to light, and only photoreceptors can initiate light responses in the outer retina. Activated photoreceptors are therefore likely to release signals that influence fluid transport in RPE cells in a light-dependent manner. Reduced light-dependent OCT changes in outer retina in stage I rd10 mice is consistent with diminished photoreceptor signal in these animals.

As retinal degeneration progresses in rd10 mice, subretinal fluid typically accumulates and becomes pathological, first in smaller regions in the posterior pole (stage II) and then in extensive contiguous areas later in degeneration (stage III). For stage II rd10 mice, the amount of subretinal fluid varied with the conditions of light adaptation (Figs. 3, 4). While subretinal fluid was clearly visible on OCT images captured from light-adapted animals, the amount was significantly reduced to the point of resolution (as in examples shown in Fig. 3B) following overnight dark-adaptation, indicating that RPE is capable to remove excess fluid in subretinal space even in this stage of retinal degeneration. The light-dependent OCT changes in stage II rd10 mice also indicate that there are still residual functional photoreceptors persisting in the retina.[18,32] On the other hand, the removal of excess fluid by dark-adaptation for stage II rd10 mice is not complete as the slope of light-dependent OCT response versus light-adapted outer retinal length is less than unity (Figs. 3D, 4D). In addition, the slope decreases with the progress of retinal degeneration, from 0.84 for P32 to P35 mice shown in Figure 3D to 0.40 for P35 to P38
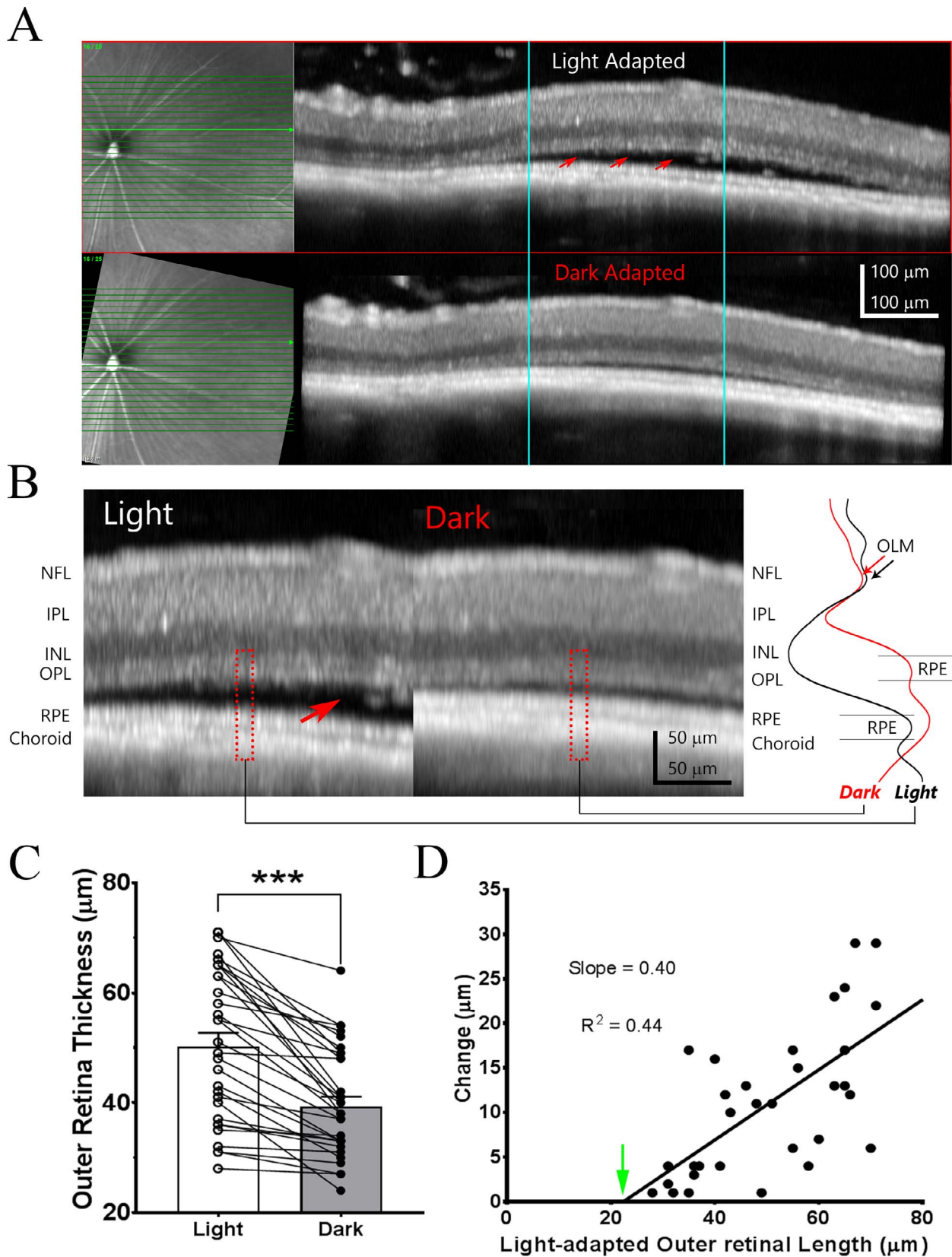
FIGURE 4. Light-adaptation induced subretinal fluid changes in stage II rd10 mice revealed by Spectralis OCT system. (A) Example of OCT images obtained from the same P38 rd10 mouse eye under light-adapted and "follow-up" exam with Spectralis OCT system after overnight dark-adaptation. Infrared fundus images are shown on the *left side* of the panel. *Red arrows* point to accumulation of subretinal fluid on OCT images acquired under light-adapted condition. (B) Side-by-side comparison of the OCT images for the same local retina region (outlined by *blue lines* in [A]). Intensity profiles for outer retina region outline by *dash red box* are shown on the *right side panel. Red arrow* points to the fluid accumulation in subretinal space under light-adapted condition, which is largely disappeared on OCT image acquired under dark-adapted condition. (C) *Bar graph* illustrates

averaged outer retinal thickness under light and dark-adapted conditions (*n* = 32). (**D**) Relationship of outer retina thickness changes and outer retinal length observed under light-adapted condition (*n* = 32 measurements from 32 eyes of 16 animals; Pearson's correlation coefficient). *Green arrow* points to *X*-intercept, a value corresponds to the outer retina length with no subretinal fluid accumulation.
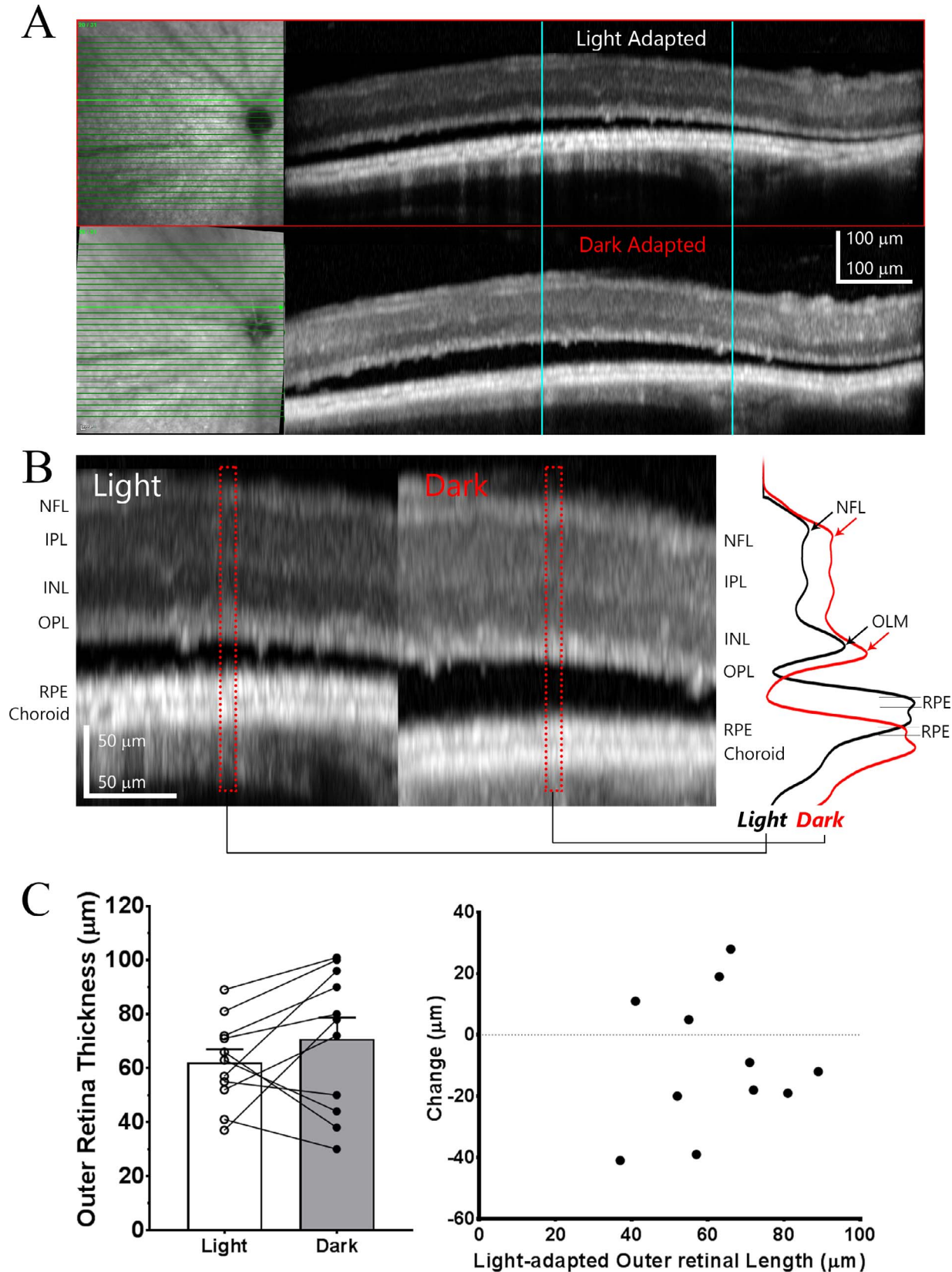

FIGURE 5. Light-adaptation has no effect on subretinal fluid in stage III rd10 mice. (**A**) Example of OCT images obtained from the same P45 rd10 mouse eye under light-adapted and "follow-up" exam after overnight dark-adaptation. Infrared fundus images are shown on the *left side* of the

panel. **(B)** Magnified OCT images for the same local retina region (outlined by *blue lines* in [A]) for side-by-side comparison. Intensity profiles of region outlined by *dash red box* are shown on the *right-side panel*. **(C)** *Bar graph* illustrates averaged outer retinal thickness under light and dark-adapted conditions ($n = 11$). **(D)** Relationship of outer retina thickness changes and outer retinal length observed under light-adapted condition.

rd10 mice shown in Figure 4D. With further retinal degenerations, stage III rd10 mice exhibited massive subretinal fluid (Fig. 5). The amount of fluids accumulated under subretinal space did not change significantly under light- and dark-adapted conditions. It is likely that the number of residual photoreceptors at this stage of rd10 retina is insufficient to regulate fluid transport in RPE cells. As rod photoreceptors degenerate, cone progressively dominate photoreceptor response in rd10 retina. The contribution of cones to light-dependent OCT response is complicated by findings that GNAT1$^{-/-}$ mice lack similar response[9] and do not show light-dependent water mobility changes in subretinal space.[14] Although there are substantial rod degeneration in rd10 retina early on, rods still outnumber cones for the time points for which the light response was evaluated, especially for stage I (P21–P26) eyes, making a rod contribution to the response still plausible.

It is interesting to note that the largest outer retina length changes over light- and dark-adaptation observed from stage II

rd10 mice reached 30 to 40 μm (Figs. 3, 4). The capacity of RPE cells for fluid transport is estimated in range of 1.4 to 11 μL/cm^2.h,[33–35] which is equivalent to a steady transport of 14 to 110 μm of fluid across the surface of RPE per hour. Therefore, the removal of 30 to 40 μm of subretinal fluid after overnight (>10 hours) dark-adaptation is well within the capacity of RPE pump activity.

It is not clear how subretinal fluid accumulates in rd10 mice with retinal degeneration. Not all retinal degeneration leads to the development of subretinal edema, as rd1 mice never develop fluid accumulation in subretinal space despite a very rapid rate of degeneration.[11] During the degeneration in rd10 mice, the outer retina is infiltrated with immune cells, including microglia cells,[24,32] which could cause tissue inflammation. It is also possible that RPE cells have a reduced pumping activity under light-adapted conditions, which leads accumulation of fluid as by-product of metabolism. As subretinal space has lower physical resistance to fluid flow,[14,28] it becomes a locus for the accumulation of excess
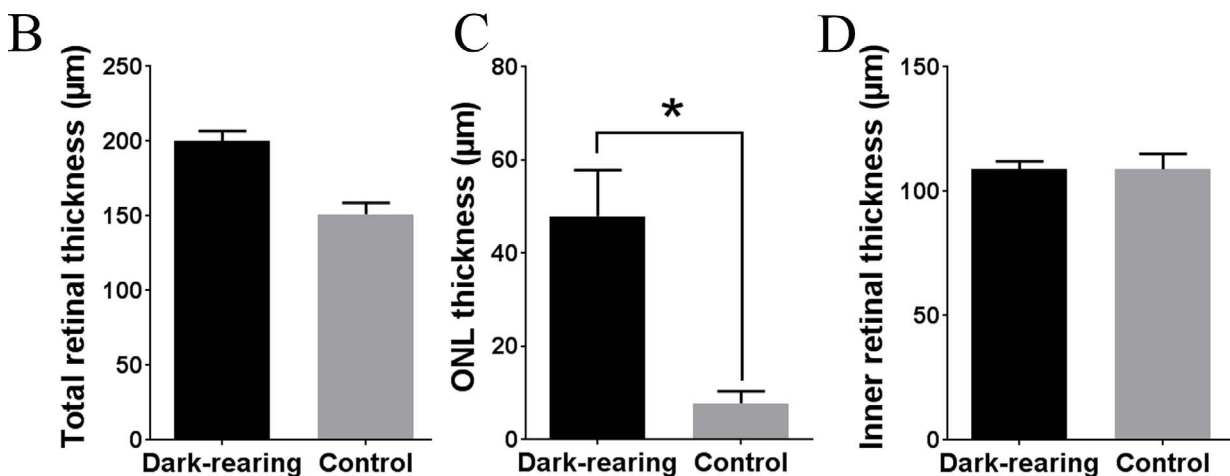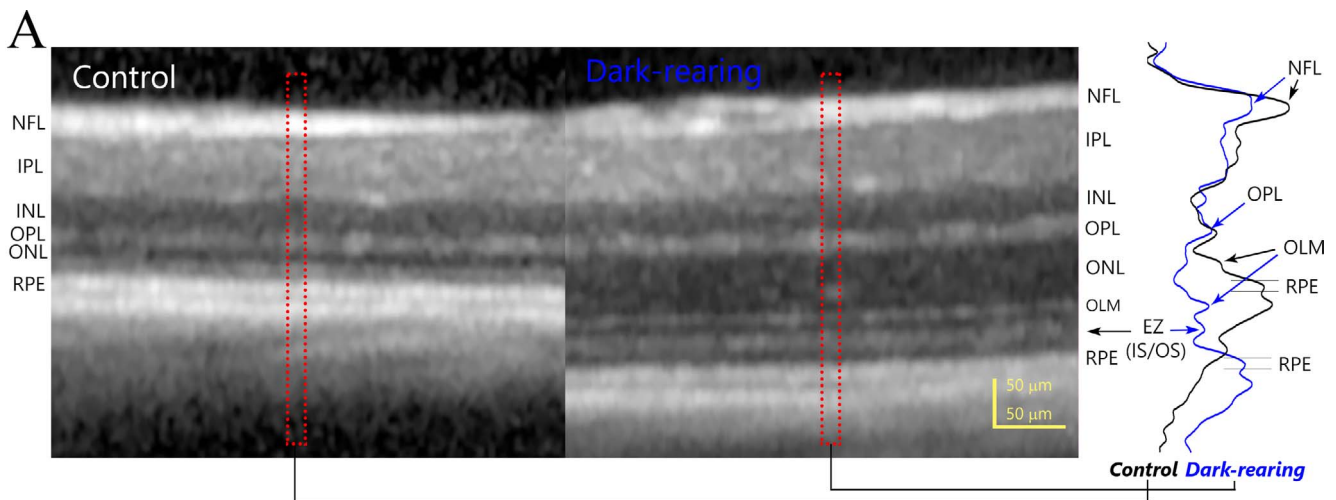
FIGURE 6. Dark rearing protects degeneration in rd10 mice. **(A)** Example of OCT images obtained from a P30 rd10 mouse raised in normal light condition (Control) and a P30 rd10 mouse raised in total darkness (Dark-rearing). Intensity profiles of region outlined by *dash red box* are shown on the *right-side panel*. **(B–D)** *Bar graph* shows averaged thickness of total retina **(B)**, ONL **(C)**, and inner retina **(D)** for rd10 mice reared in normal light cycles ($n = 4$) and those reared in total darkness ($n = 4$).

fluid in the retina. Accumulation of excess fluid in subretinal space will create a barrier for RPE and photoreceptor interaction, and prevent RPE cells from providing nutrients for photoreceptors, and thus accelerate retinal degeneration. Therefore, removing subretinal fluid will be beneficial to limiting degeneration in these animals. Our results of dark-rearing are consistent with this notion. As subretinal fluid accumulation decreases under dark-adapted conditions, dark-reared mice demonstrated better preserved outer retinal thicknesses compared with those housed under normal cyclic light condition (Fig. 6). In addition, EZ (IS/OS) zone is more prominent on OCT images obtained from dark-rearing rd10 mice, whereas the band cannot be detected on those of control rd10 mice, indicating healthier photoreceptors in the dark reared animals. Similar protective effects of dark rearing on rd10 mice have also been observed previously.[18]

Intraretinal cystic edema occurs commonly in human RP patients (10%–50%)[36] and can sometimes be complicated further by subretinal fluid accumulation.[37,38] A recent study reported similar changes in photoreceptor layer thickness induced by light flash for normal human subjects.[10] It is likely that the mechanisms in regulating subretinal fluid dynamic are similar in human and mouse eyes. Dark-adaptation could activate RPE pump, increase outflow of subretinal fluid, and be neuroprotective. Although dark rearing is not a feasible approach for human eye disease, further study to identify the responsible molecular signals could lead to therapeutic approaches that specifically modulate subretinal fluid dynamics in human patients.

References

1. Fujimoto J, Swanson E. The development, commercialization, and impact of optical coherence tomography. *Invest Ophthalmol Vis Sci*. 2016;57:OCT1–OCT13.

2. Fujimoto JG. Optical coherence tomography for ultrahigh resolution in vivo imaging. *Nat Biotechnol*. 2003;21:1361–1367.

3. Fujimoto J, Huang D. Foreword: 25 years of optical coherence tomography. *Invest Ophthalmol Vis Sci*. 2016;57:OCTi–OCTii.

4. Li Y, Fariss RN, Qian JW, Cohen ED, Qian H. Light-induced thickening of photoreceptor outer segment layer detected by ultra-high resolution OCT imaging. *Invest Ophthalmol Vis Sci*. 2016;57:OCT105–OCT111.

5. Zhang QX, Lu RW, Messinger JD, Curcio CA, Guarcello V, Yao XC. In vivo optical coherence tomography of light-driven melanosome translocation in retinal pigment epithelium. *Sci Rep*. 2013;3:2644.

6. Bizheva K, Pflug R, Hermann B, et al. Optophysiology: depth-resolved probing of retinal physiology with functional ultrahigh-resolution optical coherence tomography. *Proc Natl Acad Sci U S A*. 2006;103:5066–5071.

7. Majdi JA, Qian H, Li Y, et al. The use of time-lapse optical coherence tomography to image the effects of microapplied toxins on the retina. *Invest Ophthalmol Vis Sci*. 2015;56:587–597.

8. Abramoff MD, Mullins RF, Lee K, et al. Human photoreceptor outer segments shorten during light adaptation. *Invest Ophthalmol Vis Sci*. 2013;54:3721–3728.

9. Zhang P, Zawadzki RJ, Goswami M, et al. In vivo optophysiology reveals that G-protein activation triggers osmotic swelling and increased light scattering of rod photoreceptors. *Proc Natl Acad Sci U S A*. 2017;114:E2937–E2946.

10. Lu CD, Lee B, Schottenhamml J, Maier A, Pugh EN Jr, Fujimoto JG. Photoreceptor layer thickness changes during dark adaptation observed with ultrahigh-resolution optical coherence tomography. *Invest Ophthalmol Vis Sci*. 2017;58:4632–4643.

11. Pennesi ME, Michaels KV, Magee SS, et al. Long-term characterization of retinal degeneration in rd1 and rd10 mice using spectral domain optical coherence tomography. *Invest Ophthalmol Vis Sci*. 2012;53:4644–4656.

12. Marmor MF. Control of subretinal fluid: experimental and clinical studies. *Eye (Lond)* 1990;4(Pt 2):340–344.

13. Huang B, Karwoski CJ. Light-evoked expansion of subretinal space volume in the retina of the frog. *J Neurosci*. 1992;12:4243–4252.

14. Berkowitz BA, Grady EM, Khetarpal N, Patel A, Roberts R. Oxidative stress and light-evoked responses of the posterior segment in a mouse model of diabetic retinopathy. *Invest Ophthalmol Vis Sci*. 2015;56:606–615.

15. Li JD, Gallemore RP, Dmitriev A, Steinberg RH. Light-dependent hydration of the space surrounding photoreceptors in chick retina. *Invest Ophthalmol Vis Sci*. 1994;35:2700–2711.

16. Li JD, Govardovskii VI, Steinberg RH. Light-dependent hydration of the space surrounding photoreceptors in the cat retina. *Vis Neurosci*. 1994;11:743–752.

17. Chang B, Hawes NL, Hurd RE, Davisson MT, Nusinowitz S, Heckenlively JR. Retinal degeneration mutants in the mouse. *Vision Res*. 2002;42:517–525.

18. Chang B, Hawes NL, Pardue MT, et al. Two mouse retinal degenerations caused by missense mutations in the beta-subunit of rod cGMP phosphodiesterase gene. *Vision Res*. 2007;47:624–633.

19. Mclaughlin ME, Sandberg MA, Berson EL, Dryja TP. Recessive mutations in the gene encoding the beta-subunit of rod phosphodiesterase in patients with retinitis-pigmentosa. *Nat Genet*. 1993;4:130–134.

20. Rosch S, Johnen S, Müller F, Pfarrer C, Walter P. Correlations between ERG, OCT, and Anatomical Findings in the rd10 Mouse. *J Ophthalmol*. 2014;2014:874751.

21. Gargini C, Terzibasi E, Mazzoni F, Strettoi E. Retinal organization in the retinal degeneration 10 (rd10) mutant mouse: a morphological and ERG study. *J Comp Neurol*. 2007;500:222–238.

22. Barhoum R, Martinez-Navarrete G, Corrochano S, et al. Functional and structural modifications during retinal degeneration in the rd10 mouse. *Neuroscience*. 2008;155:698–713.

23. Pang JJ, Dai X, Boye SE, et al. Long-term retinal function and structure rescue using capsid mutant AAV8 vector in the rd10 mouse, a model of recessive retinitis pigmentosa. *Mol Ther*. 2011;19:234–242.

24. Zabel MK, Zhao L, Zhang Y, et al. Microglial phagocytosis and activation underlying photoreceptor degeneration is regulated by CX3CL1-CX3CR1 signaling in a mouse model of retinitis pigmentosa. *Glia*. 2016;64:1479–1491.

25. Jonnal RS, Kocaoglu OP, Zawadzki RJ, Lee SH, Werner JS, Miller DT. The cellular origins of the outer retinal bands in optical coherence tomography images. *Invest Ophthalmol Vis Sci*. 2014;55:7904–7918.

26. Spaide RF, Curcio CA. Anatomical correlates to the bands seen in the outer retina by optical coherence tomography: literature review and model. *Retina*. 2011;31:1609–1619.

27. Staurenghi G, Sadda S, Chakravarthy U, Spaide RF; International Nomenclature for Optical Coherence Tomography Panel. Proposed lexicon for anatomic landmarks in normal posterior

segment spectral-domain optical coherence tomography: the IN*OCT consensus. *Ophthalmology*. 2014;121:1572–1578.

28. Bissig D, Berkowitz BA. Light-dependent changes in outer retinal water diffusion in rats in vivo. *Mol Vis*. 2012;18:2561–2577.

29. Strauss O. The retinal pigment epithelium in visual function. *Physiol Rev*. 2005;85:845–881.

30. Peterson WM, Meggyesy C, Yu K, Miller SS. Extracellular ATP activates calcium signaling, ion, and fluid transport in retinal pigment epithelium. *J Neurosci*. 1997;17:2324–2337.

31. Reichhart N, Strauss O. Ion channels and transporters of the retinal pigment epithelium. *Exp Eye Res*. 2014;126:27–37.

32. Zhao L, Zabel MK, Wang X, et al. Microglial phagocytosis of living photoreceptors contributes to inherited retinal degeneration. *EMBO Mol Med*. 2015;7:1179–1197.

33. Gallemore RP, Hughes BA, Miller SS. Retinal pigment epithelial transport mechanisms and their contributions to the electroretinogram. *Prog Retin Eye Res*. 1997;16:509–566.

34. Hamann S. Molecular mechanisms of water transport in the eye. *Int Rev Cytol*. 2002;215:395–431.

35. Wimmers S, Karl MO, Strauss O. Ion channels in the RPE. *Prog Retin Eye Res*. 2007;26:263–301.

36. Bakthavatchalam M, Lai FHP, Rong SS, Ng DS, Brelen ME. Treatment of cystoid macular edema secondary to retinitis pigmentosa: a systematic review [published online ahead of print October 5, 2017]. *Surv Ophthalmol*. doi:10.1016/j.survophthal.2017.09.009.

37. Paulus YM, Wenick AS. Development of chronic subretinal fluid in Kearns-Sayre syndrome. *Retin Cases Brief Rep*. 2016;10:236–238.

38. Kozma P, Hughbanks-Wheaton DK, Locke KG, et al. Phenotypic characterization of a large family with RP10 autosomal-dominant retinitis pigmentosa: an Asp226Asn mutation in the IMPDH1 gene. *Am J Ophthalmol*. 2005;140:858–867.